CHAPTER 5

CLASSIFICATION AND PERFORMANCE EVALUATION OF PROPOSED CAD SYSTEM

5.1 INTRODUCTION

Classification deals with finding similarity between the segmentation algorithms and radiologist report. The next step after detection and segmentation of the ROI is the extraction of features that would depict the class of the tumor to which it belongs. Features are used as inputs to the classifiers. In this work similarity index is used as a classifier of the proposed CAD system. The diagnostic performance and accuracy of the computation in discriminating the diseased cases from normal case is evaluated using ROC curve.

5.2 FEATURE EXTRACTION

Feature extraction is the key step for the classification. The next step after detection and segmentation of the ROI is the extraction of features that would depict the class of the tumor to which it belongs. Features are used as inputs to the classifiers. Feature construction is the process that aims at discovering the hidden relationships between pixel values and its location and inferring new composite features. Identified suspicious regions are further analyzed and statistical features are constructed. In the statistical approach the data will be analyzed by the gray level distributions of the texture. Statistical methods analyze the spatial distribution of gray values, by computing local features at each point in the image, and deriving a set of statistics from the distributions of the local features. The reason behind this is the fact that the spatial distribution of gray values is one of the defining qualities of texture. Depending on the number of pixels defining the local feature, statistical

methods can be further classified into first order (one pixel), second-order (two pixels) and higher-order (three or more pixels) statistics (Sklansky J, 1978). The basic difference is that first-order statistics estimate properties (e.g. average and variance) of individual pixel values, ignoring the spatial interaction between image pixels, whereas second and higher order statistics estimate properties of two or more pixel values occurring at specific locations relative to each other. It has been shown that in Roberts et al., 1996 that two textures are only differentiable by human eye if they have different second order statistics. Feature construction has been achieved by second order and higher order methods.

5.2.1 Co-occurrence Method

The methods based on the Co-occurrence matrices are standard tools in texture segmentation. Gray Level Co-occurrence Matrices (GLCM) show how often each gray level occurs at a pixel located at a fixed geometric position relative to each other pixel, as a function of the gray level. The size of co-occurrence matrix will be the number of threshold levels. Figure5.1 shows 3 X 3 image and its 4 gray level co-occurrence matrices. The number of threshold levels is 4. The 2 in the co occurrence matrix indicates that there are two occurrences of a pixel with gray level 3 immediately to the right of pixel with gray level 1.When we consider neighboring pixels, the distance between the pair of pixels is 1. However, each different relative position between the two pixels to be compared creates a different co-occurrence matrix.

1	3	2
3	1	3
2	1	4

Figure5.1 a)Original Image

0	0	2	1
1	0	0	0
1	1	0	0
0	0	0	0

Figure5.1 b)Co-occurrence Matrix

Co-occurrence Matrix describes the textures by the joint probability of pairs of gray values in different locations. These probabilities are estimated by counting the number of pixels separated by an inter sample distance d, oriented by an angle θ, and having a specific combination of gray values. The result is then stored in a probability density matrix called co-occurrence matrix p.

By changing the orientation of θ and the distance d, a set of co-occurrence matrices has been created. From these co-occurrence matrices statistical features are computed for further classification. Haralick et al., 1973 introduced fourteen such features which have been used and calculated by using Equations (5.1)-(5.17).

i. Angular Second Moment $f_1 = \sum_i \sum_j \{p(i,j)\}^2$ (5.1)

ii. Contrast $f_2 = \sum_{n=0}^{N_g-1} n^2 \left\{ \sum_{i=1}^{N_g} \sum_{\substack{j=1 \\ |i-j|=n}}^{N_g} p(i,j) \right\}$ (5.2)

iii. Correlation $f_3 = \dfrac{\sum_i \sum_j (i,j)p(i,j) - \mu_x \mu_y}{\sigma_x \sigma_y}$ (5.3)

where, $\mu_x, \mu_y, \sigma_x, \sigma_y$ are the means and standard deviation of p_x and p_y.

iv. Sum of Squares (Variance) $f_4 = \sum_i \sum_j (i-\mu)^2 p(i,j)$ (5.4)

v. Inverse Difference Moment $f_5 = \sum_i \sum_j \dfrac{1}{1+(i-j)^2} p(i,j)$ (5.5)

vi. Sum Average $f_6 = \sum_{i=2}^{2N_g} i p_{x+y}(i)$ (5.6)

vii. Sum Variance $f_7 = \sum_{i=2}^{2N_g} (i-f_8)^2 p_{x+y}(i)$ (5.7)

viii. Sum Entropy $f_8 = -\sum_{i-2}^{2N_g} p_{x+y}(i) \log\{p_{x+y}(i)\}$ (5.8)

ix. Entropy $f_9 = -\sum_i \sum_j p(i,j) \log(p(i,j))$ (5.9)

x. Difference Variance f_{10} = Variance of p_{x-y} (5.10)

xi. Difference Entropy $f_{11} = -\sum_{i-0}^{N_{g-1}} p_{x-y}(i) \log\{p_{x-y}(i)\}$ (5.11)

xii. Information Measures of Correlation I :

$$f_{12} = \frac{HXY - HXY1}{\max(HX, HY)} \quad (5.12)$$

xiii. Information Measures of Correlation II:

$$f_{13} = (1 - \exp[-2.0(HXY2 - HXY)])^{1/2} \quad (5.13)$$

where, $HXY = -\sum_i \sum_j p(i,j) \log(p(i,j))$ (5.14)

where, HX and HY are entropies of p_x and p_y and

$$HXY1 = -\sum_i \sum_j p(i,j) \log\{p_x(i) p_y(j)\} \quad (5.15)$$

$$HXY2 = -\sum_i \sum_j p_x(i) p_y(j) \log\{p_x(i) p_y(j)\} \quad (5.16)$$

xiv. Maximal Correlation Coefficient:

f_{14} = (Second Largest Eigen value of Q) $^{1/2}$

where , $Q(i,j) = \sum_k \frac{p(i,k)p(j,k)}{p_x(i)\, p_y(k)}$

The texture of the images refers to the appearance, structure and arrangement of the parts of an object within the image. Images used for diagnostic purposes in clinical practice are digital. A feature value is a real

number which encodes some discriminatory information about a property of an object.

5.2.2 Gray Level Dependence Matrix (GLDM)

The texture information is contained in the GLDM whose elements are the probabilities of finding a pixel, which has gray tone i at a distance d_s and an angle ϕ from a pixel, which has gray tone j. Each pixel is considered as having eight nearest neighbors connected to it, except at the periphery. The neighbors can be grouped into four categories. The texture information is contained in GLDM P(i , j), where each P(i, j : d_s :ϕ) is the probability with which two neighboring pixels, one with gray tone i and the other with gray tone j, when separated by a distance d_s and an angle ϕ, thus a low contrast image will have a strongly diagonal matrix, with very low counts for matrix elements far from the diagonal elements. If the texture in the image is coarse, d_s 1 have similar gray levels and there will be many counts along the main diagonal of the matrix. Conversely, high variations within the image will appear in the matrix as substantial numbers of counts located from the diagonal, making the over all matrix uniform.

5.3 FEATURE SELECTION USING GA

GA is an iterative optimization process where a set of operators, such as crossover and mutation are applied. First a solution is represented by a finite sequence of 0's and 1's, called chromosome. The chromosomes are allowed to crossover by randomly choosing some point (called crossover point). Chromosomes are also allowed to mutate by flipping a bit. The optimization process is carried out in generations where each time a population of new chromosomes is generated. Since the population size is finite, only the best chromosomes are allowed to survive.

5.4 CLASSIFICATION OF SUSPICIOUS REGION IN MRI BRAIN IMAGE

Classification is often the ultimate goal especially in medical applications. Once the diagnosis is made, the physician needs a quantified data to determine the extent of progression of a disease. Salman et al., 2005 described that the true positive detection rate and the number of false positive detection rate at various thresholds of the images are used to measure the algorithm's performance.

A region extracted from the asymmetry image which overlaps with a true abnormality as provided in the ground truth of the image is called true positive detection. In the existing work Salman et al., 2005 and Leung et al., 2003 have considered 40% overlap region with the radiologists' report but in the proposed work 80% overlap with the radiologists' report is considered as true positive. If the overlap is less than 80% of the radiologists' specified region, then the corresponding image is classified as false positive.

5.5 ESSENTIALS OF ROC

To evaluate the proposed systems, the classification performance of each system has to be measured. Often the performance of the system cannot be described by a single value. ROC analysis is an analytical procedure for measuring the accuracy of the system. ROC curves show a relationship between the true- positive probability and the false-positive probability. The evaluation factor is the area under the curve. ROC has the following features.

i. The index of accuracy in ROC analysis is independent of the criterion adopted in the system for making a particular decision.

ii. ROC estimates the probability of decision outcomes of various kinds for any criterion used by the system.

iii. The ROC analysis supplies an index of the decision criterion, which reflects together the subjective probabilities and utilities that usually determine this criterion.

Kramer 1992 claims that the following assumptions are made and must be fulfilled in order to do an evaluation of a medical test.

i. The period of testing must be defined to ensure that during this period whether the patient has the disorder or not.

ii. The purpose of the medical test is to help in determining whether a patient has a specific disorder during the period of testing or not.

iii. The diagnosis of the disorder used to evaluate a medical test must be clinically valid

5.6 SIMILARITY INDEX

The performance of the CAD system is best described in terms of their similarity indices (Dice 1945) such as pixel accuracy, position accuracy, and overall accuracy by quantifying their performance related to false positive and false negative instance. These metrics are based on the consideration that a test point always falls into one of the following ROC parameters.

- False Positive (FP)
- False Negative (FN)
- True Positive (TP)
- True Negative (TN)

Table 5.1 ROC Parameter and its Justification

Parameter	Justification
True Positive (TP)	Tumor marked as malignant which is also classified as tumor.
True Negative (TN)	Tumor which are neither marked as malignant nor classified as malignant.
False Positive (FP)	Tumor which are not marked as tumor but classified as tumor.
False Negative (FN)	Tumor which are marked as tumor but not classified as tumor.

5.6.1 Pixel Accuracy

To compare the manual segmented pixel with the system segmented pixels, pixel accuracy is calculated by Equation (5.16).

$$\text{Pixel Accuracy (\%)} = [2(A \cap B)/ (A+B)] \text{ X } 100 \qquad (5.16)$$

where, A = Number of segmented pixel by radiologist

B = Number of segmented pixel by CAD system

$A \cap B$ – Common number of pixels segmented by the radiologist and CAD system.

A+B – Total number of segmented pixels by the radiologist and CAD system.

5.6.2 Position Accuracy

To calculate similarity between the radiologists's segmented tumor position with CAD system segmented tumor position, it is essential to find the

accuracy of the pixel position level which is calculated by using Equation (5.17).

$$\text{Position Accuracy} = \left.\begin{array}{l} \text{X Starting Position Accuracy (25\%)} + \\ \text{X Ending Position Accuracy (25\%)} + \\ \text{Y Starting Position Accuracy (25\%)} + \\ \text{Y Ending Position Accuracy (25\%)} \end{array}\right\} \quad (5.17)$$

5.6.3 Overall Accuracy

In this work, the tumor pixel accuracy with weight 75% and position accuracy with weight 25% is considered because the number of tumor segmented pixel should have more accuracy than the position accuracy. Overall system accuracy is calculated by using Equation (5.18).

$$\text{Overall Accuracy} = 75\% \text{ (Pixel accuracy)} + 25\% \text{ (Position accuracy)} \quad (5.18)$$

5.7 PERFORMANCE ANALYSIS OF THE CLASSIFICATION SYSTEM

In the proposed system the spatial coordinate position of the suspicious region (x, y) and the radius of the suspicious region are determined by using efficient algorithms. The number of pixels in the suspicious region within the radius is calculated. On comparing the number of the segmented pixels in the resultant asymmetry image at (x, y) position with the predefined radiologist report, the classification is made. Figure 5.3 depicts asymmetry image at (x, y) position.

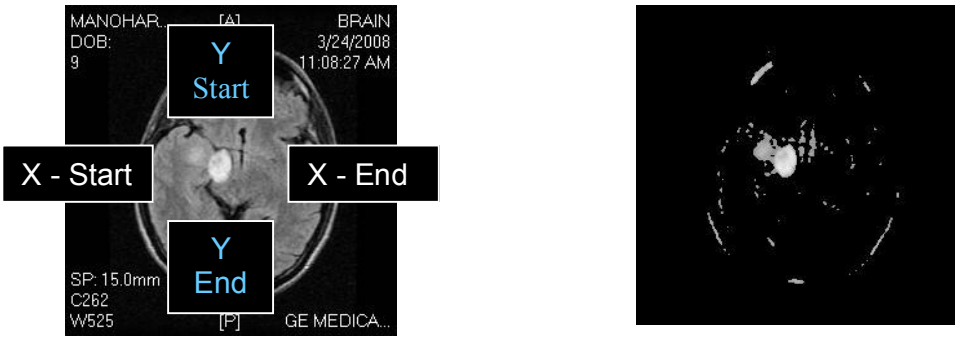

(a) (b)

Figure 5.2 (a) Asymmetry Image at (x, y) Position
(b) Detection of Tumor Pixels

On comparing the obtained test results with the radiologist's report, the proposed method overlaps 98% of the specified suspicious region and this image is classified as true positive image. In case the overlap is less than the fixed 80% of the specified region, the image is considered as false positive image.

For example, the radiologists' report for the MRI brain image named Geetha. jpg, the spatial coordinate position of the suspicious region x and y are (97,130) respectively and the radius is 42. In this specified region the maximum available pixels are 1764, in which the radiologists' report has specified 1240 pixels are tumor pixels. Table5.1 describes the radiologists' report for randomly selected 10 patients' MRI brain image.

The details of the segmented suspicious region of the same image by various proposed techniques are as follows: (i) RRS with GA method contains spatial co ordinates at (56, 79) with 461 pixels. (ii) NRRS with GA contains spatial co ordinate at (50, 72) with 1006 pixels. (iii) MRF-MAP-PACO contains spatial co ordinate at (97,130) with 1240 segmented pixels.

Hence the classification is made based on the pixel similarity and position similarity.

5.7.1 Performance Evaluation of Proposed CAD System

Performance evaluations determine how well a system performs relative to some required results. To evaluate the constructed system, the classification performance of each proposed system has to be measured. In this thesis the ROC parameters TP, TN, FP and FN are found and further the quality of the system is measured in terms of sensitivity (SE), specificity (SP), efficiency (EFF) and error rate.

Sensitivity (SE) is the probability of having a positive test among the patients who have a positive diagnosis. Sensitivity is the ratio of tumors that were marked and classified as tumor to all unmarked tumors given by Equation (5.19). Specificity is the ratio of tumors that were not marked as tumor and also not classified as tumor to all unmarked tumors. It is calculated using Equation (5.20). Efficiency is calculated using Equation (5.21).

$$SE = TP / (TP+FN \tag{5.19}$$

$$SP = TN / (FP+TN) \tag{5.20}$$

$$EFF = TP + TN \tag{5.21}$$

The total area under the ROC curve is referred to as A_z value. It is the measure of the classification performance since it reflects the test performance at all possible cut-off levels. The area lies in the interval [0.5-1] and the larger this area, the better the performance of the classification. In this work A_z value is used to compare the results of the proposed metaheuristic algorithms. Figure 5.4 depicts the ROC performance analysis and it explains that the classification accuracy by PSI based classifier is 0.9869 which is much better than the other classifiers.

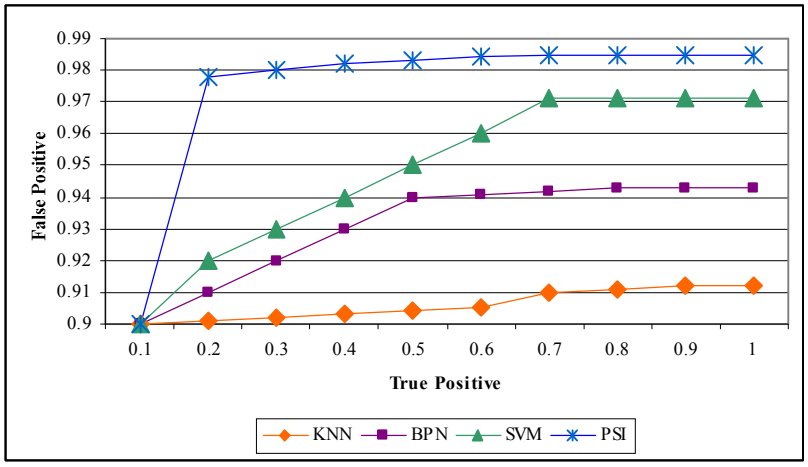

Figure 5.3 ROC Analysis

To validate the findings and compare the results of the simulated brain images with the real times images, 100 patients' detail are randomly selected from the real time MRI brain image database from KMCH. The algorithms have been tested on the real time images. Tables 5.2-5.14 explain the computational results for the real times MRI brain images.

Table 5 .2 Radiologist Report

ID No.	Image Name	Images	X Position	Y Position	Radius	No.of Seg.Pixels	Classification
51	Geetha.jpg	Target 1	97	143	42	1240	TP
40	Kandhasamy.jpg	Target 2	92	181	36	866	TP
35	Lakshmi. Jpg	Target 3	121	120	80	2989	TN
4	Leela. Jpg	Target 4	132	137	19	397	TN
39	Manoharan. Jpg	Target 5	104	141	64	2121	TP
41	Shameema. Jpg	Target 6	132	145	100	1304	TN
7	Somin1. Jpg	Target 7	121	125	28	494	TN
37	Tumin. Jpg	Target 8	148	147	24	354	TP
36	Veni.jpg	Target 9	134	130	80	1606	TN
50	Vidhya.jpg	Target 10	128	106	42	674	TP

Table 5.3 Results of RRS – GA Technique

ID No.	Image Name	Images	X Position	Y Position	Radius	No.of Seg.Pixels	Classification
51	Geetha.jpg	Target 1	56	79	38	461	TP
40	Kandhasamy.jpg	Target 2	78	102	36	992	TP
35	Lakshmi. Jpg	Target 3	80	108	77	979	FP
4	Leela. Jpg	Target 4	110	124	15	275	TN
39	Manoharan. Jpg	Target 5	90	139	62	1138	TP
41	Shameema. Jpg	Target 6	111	121	102	441	TN
7	Somin1. Jpg	Target 7	102	102	29	245	TN
37	Tumin. Jpg	Target 8	124	115	18	622	TP
36	Veni.jpg	Target 9	131	122	80	410	FP
50	Vidhya.jpg	Target 10	110	67	40	514	TP

Table 5.4 Results of NRRS – GA Technique

ID No.	Image Name	Images	X Position	Y Position	Radius	No.of Seg.Pixels	Classification
51	Geetha.jpg	Target 1	50	72	36	1006	TP
40	Kandhasamy.jpg	Target 2	65	56	34	1015	TP
35	Lakshmi. Jpg	Target 3	73	107	77	1248	FP
4	Leela. Jpg	Target 4	111	126	18	633	TN
39	Manoharan. Jpg	Target 5	74	127	60	918	TP
41	Shameema. Jpg	Target 6	94	98	100	935	FP
7	Somin1. Jpg	Target 7	101	67	27	774	TN
37	Tumin. Jpg	Target 8	118	109	20	937	TP
36	Veni.jpg	Target 9	95	114	81	1218	FP
50	Vidhya.jpg	Target 10	89	73	37	888	FN

Table 5.5 Results of MRF-MAP-PACO Segmentation

ID No.	Image Name	Images	X Position	Y Position	Radius	No.of Seg.Pixels	Classification
51	Geetha.jpg	Target 1	97	130	42	1240	TP
40	Kandhasamy.jpg	Target 2	95	181	36	866	TP
35	Lakshmi. Jpg	Target 3	121	120	80	2989	TN
4	Leela. Jpg	Target 4	132	137	19	397	TN
39	Manoharan. Jpg	Target 5	100	129	64	2121	TP
41	Shameema. Jpg	Target 6	124	126	100	1304	TN
7	Somin1. Jpg	Target 7	118	123	28	494	TN
37	Tumin. Jpg	Target 8	148	147	24	354	TP
36	Veni.jpg	Target 9	134	133	80	1606	TN
50	Vidhya.jpg	Target 10	128	106	42	674	FP

Table 5.6 Pixel Accuracy of RRS – GA Technique

ID No.	Image Name	Images	RRS with GA	Manual	Pixel Accuracy
51	Geetha.jpg	Target 1	461	1240	37.17
40	Kandhasamy.jpg	Target 2	992	866	87.29
35	Lakshmi. Jpg	Target 3	979	2989	32.75
4	Leela. Jpg	Target 4	275	397	69.26
39	Manoharan. Jpg	Target 5	1138	2121	53.65
41	Shameema. Jpg	Target 6	441	1304	33.81
7	Somin1. Jpg	Target 7	245	494	49.59
37	Tumin. Jpg	Target 8	622	354	56.91
36	Veni.jpg	Target 9	410	1606	25.52
50	Vidhya.jpg	Target 10	514	674	76.26
				Average	**55.22**

Table 5.7 Position Accuracy of RRS – GA Technique

ID No.	Image Name	Images	Pixel Position						
			RRS with GA		Manual		X position Accuracy	Y position Accuracy	Position Accuracy
			X	Y	X	Y			
51	Geetha.jpg	Target 1	50	72	97	143	51.55	50.35	50.95
40	Kandhasamy.jpg	Target 2	65	56	92	181	70.65	30.94	50.80
35	Lakshmi. Jpg	Target 3	73	107	121	120	60.33	89.17	74.75
4	Leela. Jpg	Target 4	111	126	132	137	84.09	91.97	88.03
39	Manoharan. Jpg	Target 5	74	127	104	141	71.15	90.07	80.61
41	Shameema. Jpg	Target 6	94	98	132	145	71.21	67.59	69.40
7	Somin1. Jpg	Target 7	101	67	121	125	83.47	53.60	68.54
37	Tumin. Jpg	Target 8	118	109	148	147	79.73	74.15	76.94
36	Veni. Jpg	Target 9	95	114	134	130	70.90	87.69	79.29
50	Vidhya. Jpg	Target 10	89	73	128	106	69.53	68.87	69.20
Average Pixel Position Accuracy							**71.26**	**70.44**	**70.85**

Table 5.8 Overall of Accuracy of RRS – GA Technique

ID	Image Name	Images	Pixel Accuracy	Position Accuracy	Overall Accuracy
27	Geetha.jpg	Target 1	37.17	50.95	43.91
42	Kandhasamy.jpg	Target 2	87.29	50.80	83.11
53	Lakshmi. Jpg	Target 3	32.75	74.75	44.07
58	Leela. Jpg	Target 4	69.26	88.03	94.35
60	Manoharan. Jpg	Target 5	53.65	80.61	45.13
63	Shameema. Jpg	Target 6	33.81	69.40	35.03
69	Somin1. Jpg	Target 7	49.59	68.54	90.73
72	Tumin. Jpg	Target 8	56.91	76.94	53.94
89	Veni. Jpg	Target 9	25.52	79.29	36.79
93	Vidhya. Jpg	Target 10	76.26	69.20	70.28
Average			**55.22**	**70.85**	**63.03**

Table 5.9 Pixel Accuracy of NRRS – GA Technique

ID No.	Image Name	Images	NRRS with GA	Manual	Pixel Accuracy
51	Geetha.jpg	Target 1	1006	1240	81.12
40	Kandhasamy.jpg	Target 2	1015	866	85.32
35	Lakshmi. Jpg	Target 3	1248	2989	41.75
4	Leela. Jpg	Target 4	633	397	62.71
39	Manoharan. Jpg	Target 5	918	2121	43.28
41	Shameema. Jpg	Target 6	935	1304	71.70
7	Somin1. Jpg	Target 7	774	494	63.82
37	Tumin. Jpg	Target 8	937	354	37.78
36	Veni.jpg	Target 9	1218	1606	75.84
50	Vidhya.jpg	Target 10	888	674	75.90
				Average	**63.92**

Table 5.10 Position Accuracy of NRRS – GA Technique

ID No.	Image Name	Images	Pixel Position						
			NRRS with GA		Manual		X position Accuracy	Y position Accuracy	Position Accuracy
			X	Y	X	Y			
51	Geetha.jpg	Target 1	56	79	97	112	57.73	70.54	64.13
40	Kandhasamy.jpg	Target 2	78	102	92	181	84.78	56.35	70.57
35	Lakshmi. Jpg	Target 3	80	108	121	120	66.12	90.00	78.06
4	Leela. Jpg	Target 4	110	124	132	137	83.33	90.51	86.92
39	Manoharan. Jpg	Target 5	90	139	104	141	86.54	98.58	92.56
41	Shameema. Jpg	Target 6	111	121	132	145	84.09	83.45	83.77
7	Somin1. Jpg	Target 7	102	102	121	125	84.30	81.60	82.95
37	Tumin. Jpg	Target 8	124	115	148	147	83.78	78.23	81.01
36	Veni. Jpg	Target 9	131	122	134	130	97.76	93.85	95.80
50	Vidhya. Jpg	Target 10	110	67	128	106	85.94	63.21	74.57
Average Pixel Position Accuracy							**81.44**	**80.63**	**81.03**

Table 5.11 Overall Accuracy of NRRS – GA Technique

ID	Image Name	Images	Pixel Accuracy	Position Accuracy	Overall Accuracy
27	Geetha.jpg	Target 1	81.12	64.13	73.57
42	Kandhasamy.jpg	Target 2	85.32	70.57	76.69
53	Lakshmi. Jpg	Target 3	41.75	78.06	50.00
58	Leela. Jpg	Target 4	62.71	86.92	69.04
60	Manoharan. Jpg	Target 5	43.28	92.56	52.61
63	Shameema. Jpg	Target 6	71.70	83.77	71.12
69	Somin1. Jpg	Target 7	63.82	82.95	65.00
72	Tumin. Jpg	Target 8	37.78	81.01	47.57
89	Veni. Jpg	Target 9	75.84	95.80	76.70
93	Vidhya. Jpg	Target 10	75.90	74.57	74.22
Average			**63.92**	**81.03**	**72.47**

Table 5.12 Pixel Accuracy of MRF-MAP-PACO

ID No.	Image Name	Images	PACO	Manual	Pixel Accuracy
51	Geetha.jpg	Target 1	1240	1026	82.74
40	Kandhasamy.jpg	Target 2	865	866	99.88
35	Lakshmi. Jpg	Target 3	2987	2989	99.93
4	Leela. Jpg	Target 4	390	397	98.24
39	Manoharan. Jpg	Target 5	2121	2121	100.00
41	Shameema. Jpg	Target 6	1304	1304	100.00
7	Somin1. Jpg	Target 7	480	494	97.17
37	Tumin. Jpg	Target 8	354	354	100.00
36	Veni.jpg	Target 9	1606	1606	100.00
50	Vidhya.jpg	Target 10	674	674	100.00
				Average	**97.796**

Table 5.13 Position Accuracy of MRF-MAP-PACO

ID No.	Image Name	Images	Pixel Position						
			PACO		Manual		X position Accuracy	Y position Accuracy	Position Accuracy
			X	Y	X	Y			
51	Geetha.jpg	Target 1	97	130	97	143	100.00	90.91	95.45
40	Kandhasamy.jpg	Target 2	91	181	92	181	98.91	100.00	99.46
35	Lakshmi. Jpg	Target 3	121	119	121	120	100.00	99.17	99.58
4	Leela. Jpg	Target 4	126	137	132	137	95.45	100.00	97.73
39	Manoharan. Jpg	Target 5	100	129	104	141	96.15	91.49	93.82
41	Shameema. Jpg	Target 6	124	126	132	145	93.94	86.90	90.42
7	Somin1. Jpg	Target 7	118	123	121	125	97.52	98.40	97.96
37	Tumin. Jpg	Target 8	148	142	148	147	100.00	96.60	98.30
36	Veni. Jpg	Target 9	123	123	134	130	91.79	94.62	93.20
50	Vidhya. Jpg	Target 10	128	106	128	106	100.00	100.00	100.00
Average Pixel Position Accuracy							**97.38**	**95.81**	**96.59**

Table 5.14 Overall Accuracy of MRF-MAP-PACO

ID	Image Name	Images	Pixel Accuracy	Position Accuracy	Overall Accuracy
27	Geetha.jpg	Target 1	95.45	95.45	98.86
42	Kandhasamy.jpg	Target 2	99.46	99.46	99.78
53	Lakshmi. Jpg	Target 3	99.58	99.58	99.84
58	Leela. Jpg	Target 4	97.73	97.73	98.11
60	Manoharan. Jpg	Target 5	93.82	93.82	98.46
63	Shameema. Jpg	Target 6	90.42	90.42	97.60
69	Somin1. Jpg	Target 7	97.96	97.96	97.37
72	Tumin. Jpg	Target 8	98.30	98.30	99.58
89	Veni. Jpg	Target 9	93.20	93.20	98.30
93	Vidhya. Jpg	Target 10	100.00	100.00	100.00
Average			**97.79**	**96.59**	**96.89**

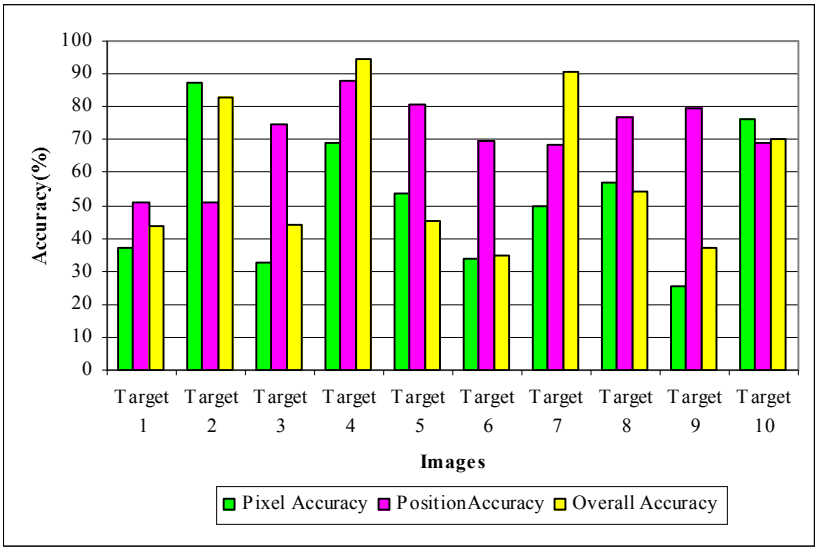

Figure 5.4 Comparison of Classification Accuracy for Bilateral Image Seg. RRS-GA Technique

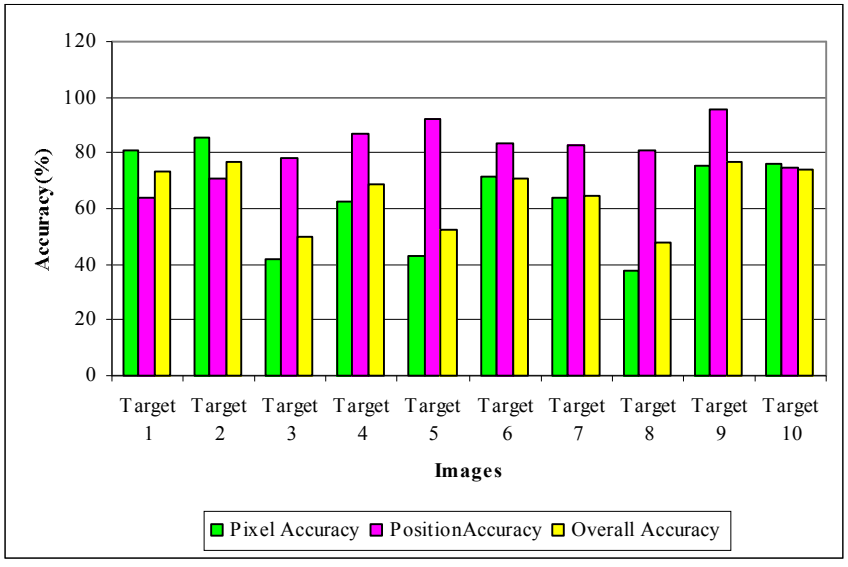

Figure 5.5 Comparison of Classification Accuracy for Bilateral Image Seg. RRS-GA Technique

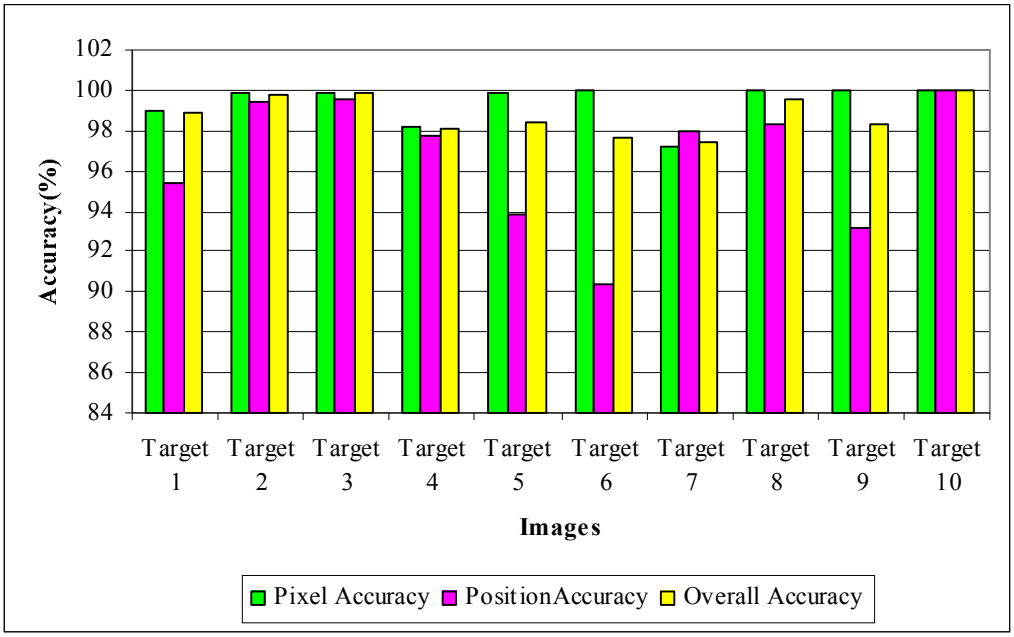

Figure 5.6 Comparison of Classification Accuracy for Single Image Seg.- MRF-MAP-PACO Technique

The above figure 5.4-5.6 describes the classification accuracy of the proposed and implemented systems in terms of pixel accuracy, position accuracy and overall accuracy. It is observed that the tumor position accuracy influences much in determining the overall accuracy than that of the pixel accuracy. The following figures 5.7-5.10 show the screen shot of ROC analysis of segmentation using MRF-MAP-PACO method.

Figure 5.7 Screenshot of ROC Analysis -with Original Image

Figure 5.8 Screenshot of ROC Analysis with Segmented Details

Figure 5.9 Screenshot of ROC Analysis -with Radiologist details and Segmented Details

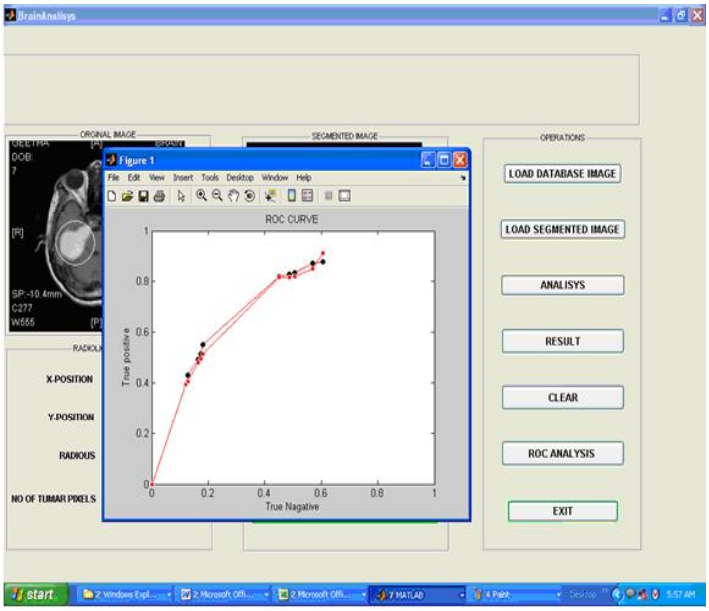

Figure 5.10 Screenshot of ROC Analysis

Table 5.15 Performance Analysis of CAD System based on Various Parameters

Methods/Parameters	RRS with GA	NRRS with GA	MRF-MAP-PACO
Execution Time(Sec)	17.2	20.5	10.6
Adaptive Threshold value	122	139	120
No.of Segmented Pixels	461	1006	1026
Pixel Accuracy (%)	55.22	63.92	99.52
Position Accuracy (%)	70.85	81.03	96.59
Overall Accuracy (%)	63.03	72.47	96.89
Error Rate (%)	0.31	0.34	0.02

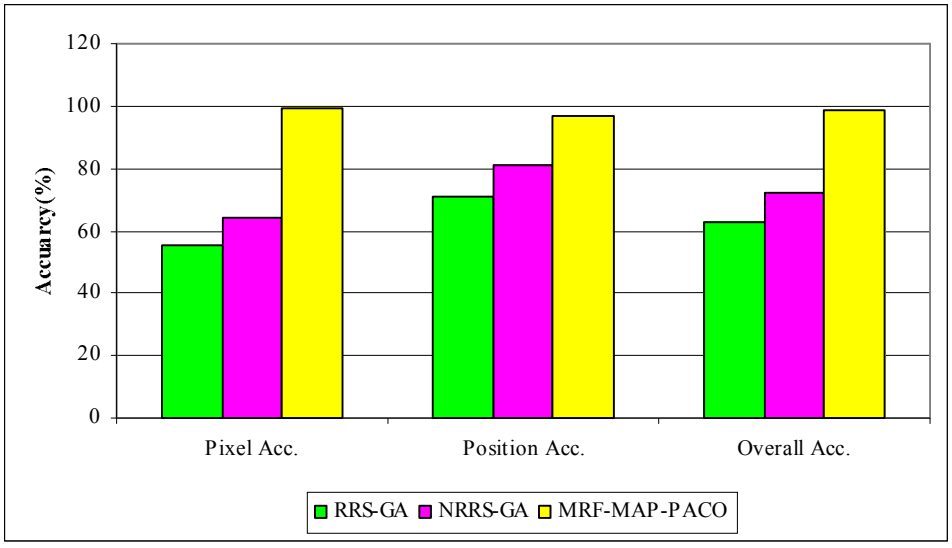

Figure 5.11 Comparison of Accuracy

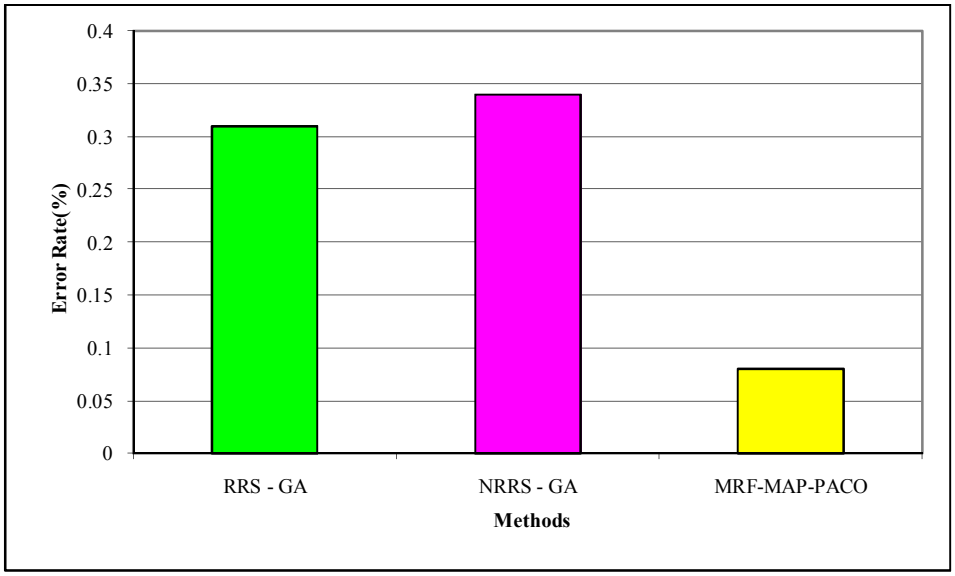

Figure 5.12 Comparison of Error Rate

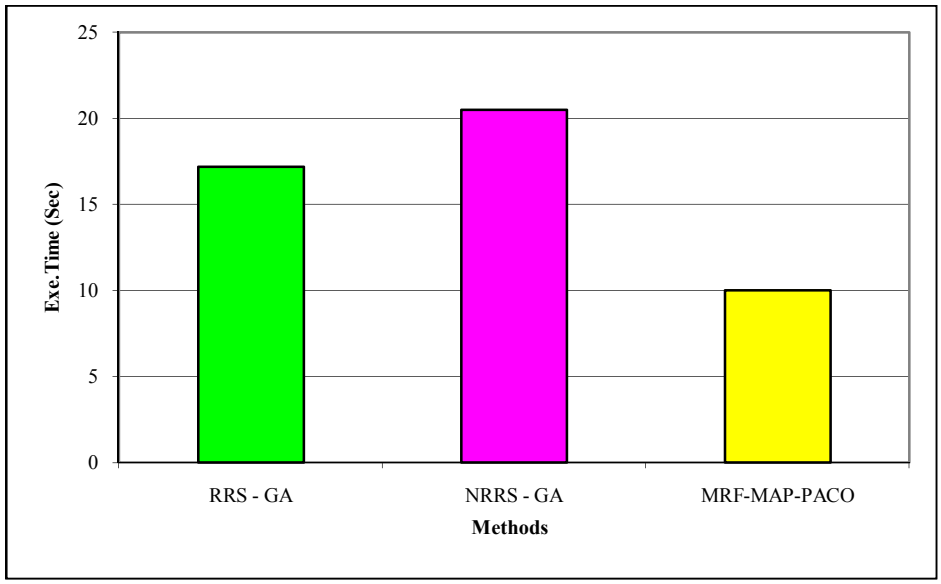

Figure 5.13 Comparison of Execution Time

Table 5.16 Comparative Performance Analysis of Classification Accuracy

Methods	Author	Classification Accuracy (%)
Texture based SI classifier	Mohsen Ghazel et al., 2006	71.84
SOM	Vijayakumar et al., 2007	86
SI based. Multi atlas based	Xabier Artaechevarria et al., 2009	75.8 85.1
PSO –SVM	Satish Chandra et al., 2009	94.42
K-means	Arpita Das et al., 2009	86
GA-SVM	Ahmed Kharrat et al., 2010	94.44
MRF-MAP-PACO-PSI	Proposed Method	96.89

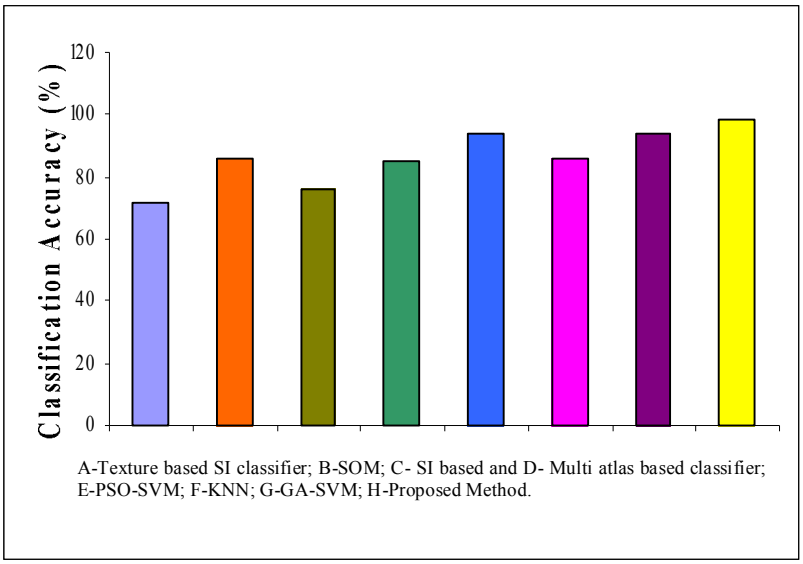

Figure 5.14 Comparative Performance Analysis of proposed Classification Method with Existing Approaches in terms of Classification Accuracy

Based on the analysis presented in this chapter, the paper entitled "Implementation of Classification System for Medical Images" in the European

Journal of Scientific Research, Vol. 53, No. 4, pp.561-569, 2011. (ISSN:1450-216X).

5.8 CONCLUSION

The computational values of classification performance measures recorded for different images have been analyzed. Performance characteristics curves with regard to pixel accuracy, position accuracy and overall accuracy of the ROI have been drawn for analysis of various target images and it is evident that the increase in the pixel accuracy of the ROI increases the overall classification accuracy of the CAD system. The simulation results show that the pixel accuracy of RRS-GA, NRRS- GA and PACO are 55.22%, 63.92% and 99.52% respectively. The position accuracy of RRS-GA, NRRS-GA and PACO are 70.85%, 81.03% and 96.59% respectively. The proposed CAD system with MRF-MAP-PACO- PSI classifier has achieved overall accuracy of 96.89% which is approximately 5% more than the other approaches such as SI classifier, SOM, Multi Atlas based classifier, PSO-SVM, KNN and GA-SVM with accuracies of 71.84%, 86%, 85.1%, 94.42%, 86% and 94.44% respectively. On comparing the investigation results with the existing systems the proposed CAD system based on ACWM-MRF-MAP-PACO-PSI classifier has achieved an overall accuracy of 96.89% which is approximately 5% more than the other existing approaches. From the investigation results, it is evident that the pixel similarity has got the superior role in determining the overall accuracy. The proposed approach has got the highest execution speed of 10sec. It is also inferred that the classification error rate introduced by the proposed approach is 0.06% -0.01% which is very minimal. The details of the computational results of the proposed scheme depicted in this chapter are also available in the paper published.